BULLETIN OF THE POLISH ACADEMY OF SCIENCES
TECHNICAL SCIENCES
Vol. 55, No. 1, 2007

Stress state analysis of harmonic drive elements by FEM

W. OSTAPSKI[1]*, and I. MUKHA[2]

[1]Institute of Machine Design Fundamentals, Warsaw University of Technology,
84 Narbutta St., 02-524 Warsaw, Poland
[2]Faculty of Applied Mathematics, Lviv University,
1 University St., 29-000 Lviv, Ukraine

Abstract. In the paper, a solution to the problem of elastic deformation of thin-walled shell structures with complex shapes within the theory of geometrically non-linear shells has been presented. It is a modification of the Newton-Raphson method. In a variational formulation, the problem is based on a Lagrange's functional for increments of displacements. The method has been applied to investigations of a harmonic drive, in particular to analysis of the stress state in the flexspline with a variable curvature as well as bearings of the generator. For verification of the obtained results, a more adequate FEM model calculated by ANSYS has been used.

Key words: FEM, thin-walled shell structures, gear of harmonic drive, mathematical modelling, stress analysis.

1. Introduction

In the paper, solution to the problem of elastic deformation of thin-walled shell structures with complex shapes within the theory of geometrically non-linear shells has been presented. The problem is up-to-date in view of practical engineering needs in the field of strength calculus of shell structures with compound shapes.

The theory of shells has proved to be quite successful both at the stage of fundamental studies on constitutive relationships as well as in examinations of given structures and prototypes. Admittedly, that success is rather related to shells of canonical forms, the middle surface of which are cylindrical, conical, spherical or any other rotational surface in general. In the engineering practice, outside of the above mentioned shells, one can come across other designs of thin-walled shells with more complex shapes.

The most widespread method of calculating shell structures, especially those of complex shapes, is FEM at the moment [1]. One can distinguish two main approaches towards the problems of theory of shells using FEM. The first one explores the on a two-dimensional shell problem. Geometry of a shell and an unknown field of displacements and angular displacements are determined by interpolating functions on a finite element. The approximation of geometry on a given element produces however greater errors than the errors of approximation of functions, which are being sought.

The second approach deals with the two-dimensional problem as well, but this time it is described in an appropriate curvilinear co-ordinate system fixed to the middle surface. In this case, it is assumed that the shell geometry is fully defined (the middle surface is described by parametric equations).

2. Parametrisation method for FE stress

Consider a parameterisation of the middle surface by making use of Monge's surfaces obtained via motion of a certain generatrix along a plane directional curve. Let the directional curve of the given surface be a curve expressed by the vector:

$$\vec{r}_0(\alpha_2) = x_1(\alpha_2)\vec{e}_1 + x_2(\alpha_2)\vec{e}_2. \tag{1}$$

Denote now by ν the unit vector of the principal direction normal to curve (1). The equation of the generatrix $\xi_1 = \xi_1(\alpha_1)$, $\xi_2 = \xi_2(\alpha_1)$ is then represented in a local co-ordinate system lying in the plane normal to the directional curve. The vector equation of the Monge surface can now be written in the form:

$$\vec{r}(\alpha_1, \alpha_2) = \vec{r}_0(\alpha_2) + \xi_1(\alpha_1)\vec{\nu}(\alpha_2) + \xi_2(\alpha_1)\vec{e}_3. \tag{2}$$

In the general case, if the given curves of the Monge surfaces are arbitrary (not given in an analytical form), it is convenient to use 'stitch' approximating functions for their parameterisation. These functions are second-order differentiable in the nodes of stitching (interpolation), and they ensure convexity and concavity conditions for the approximated curve [2].

A rapid development of non-linear theories of shells took place when much attention was paid to the solution of stability problems of thin-walled structures [3]. A sufficiently complete analysis of different variants of geometrically non-linear theories was presented in [4]. A widespread method of linearisation of non-linear problems is the Newton-Raphson method [5]. Its modification for applications to problems of elastic deformation of shells with complex shapes was discussed in [6,7].

*e-mail: wos@simr.pw.edu.pl

In a variational formulation, the considered problem is based on a Lagrange's functional for increments of displacements. It is assumed that deformation of a thin-walled shell is small, and the bending moderate.

A linear form of the hypothesis of deformation of the fibre normal to the middle surface is applied:

$$\begin{aligned} &U_s(\alpha_1,\alpha_2,\alpha_3) = u_s(\alpha_1,\alpha_2) + \alpha_3\gamma_s(\alpha_1,\alpha_2), \quad s=1,2\\ &U_3(\alpha_1,\alpha_2,\alpha_3) = u_3(\alpha_1,\alpha_2). \end{aligned} \tag{3}$$

where:
α_i – curvilinear co-ordinates to which the middle shell surface is referred,
u_1, u_2, u_3 – displacements of points of the middle surface,
γ_1, γ_2 – angular displacements of the normal direction.

The expressions for linear deformations e_{ij}, k_{rs} and angular displacements ω_{r3}, τ_{r3} are given as:

$$\begin{aligned} &e_{rs} = \frac{1}{2A_rA_s}[\nabla_s(A_ru_r) + \nabla_r(A_su_s)] + K_r\delta^s_r u_3;\\ &e_{r3} = \frac{1}{2}\left(\gamma_r + \frac{1}{A_r}\partial_r u_3 - K_r u_r\right); \quad k_{rr} = \frac{1}{A_r^2}\nabla_r(A_r\gamma_r);\\ &k_{12} = \frac{1}{2A_1A_2}\\ &\times[\nabla_2(A_1\gamma_1) + \nabla_1(A_2\gamma_2) + K_1\nabla_2(A_1u_1) + K_2\nabla_1(A_2u_2)]\\ &\omega_{r3} = \frac{1}{2}\left(\gamma_r - \frac{1}{A_r}\partial_r u_3 + K_r u_r\right); \quad \tau_{r3} = K_r\gamma_r. \end{aligned} \tag{4}$$

where: K_i are the principal curvatures of the middle surface, $r,s = 1,2$. The relationship between the derived quantities with the elements of tensors of linear and angular displacements have the following form in a 3D theory of deformation:

$$E_{rr} = \frac{e_{rr} + \alpha_3 k_{rr}}{1+\alpha_3K_r}, \quad E_{12} = \frac{e_{12}+\alpha_3k_{12}}{(1+\alpha_3K_1)(1+\alpha_3K_2)},$$

$$E_{r3} = \frac{e_{r3}}{1+\alpha_3K_r}, \quad \Omega_{r3} = \frac{\omega_{r3}+\alpha_3\tau_{r3}}{1+\alpha_3K_r}. \tag{5}$$

The components of Green's strains ε_{ij} and κ_{rs} expressed by e_{ij}, k_{rs} and ω_{r3}, τ_{r3} are as follows:

$$\varepsilon_{rs=}e_{rs} + \frac{1}{2}\omega_{r3}\omega_{s3}; \quad \varepsilon_{r3} = e_{r3};$$

$$\kappa_{rs} = k_{rs} + \frac{1}{2}(\omega_{r3}\tau_{s3} + \omega_{s3}\tau_{r3}) - \frac{1}{2}\omega_{r3}\omega_{s3}\delta^s_r K_r. \tag{6}$$

The Lagrange functional for the increments of linear and angular displacements can now be presented in the form:

$$\begin{aligned} L^{\Delta}(\Delta u,\Delta\gamma) &= \sum_m \Bigg\{ \frac{1}{2}\int_{\Omega_m} N_{rs}\Delta\omega_{r3}\Delta\omega_{s3}d\Omega\\ &+\frac{1}{2}\int_{\Omega_m} M_{rs}(\Delta\omega_{r3}\Delta\tau_{s3} + \Delta\omega_{s3}\Delta\tau_{r3} - \Delta\omega_{r3}\Delta\omega_{s3}\delta^s_rK_r)d\Omega\\ &+\frac{1}{2}\int_{\Omega_m}\left(\Delta e_{ij} + \frac{1}{2}\Delta\omega_{i3}\omega_{j3} + \frac{1}{2}\omega_{i3}\Delta\omega_{j3} + \underline{\frac{1}{2}\Delta\omega_{i3}\Delta\omega_{j3}}\right)\\ &\times A_{ijkl}\\ &\times\left(\Delta e_{kl} + \frac{1}{2}\Delta\omega_{k3}\omega_{l3} + \frac{1}{2}\omega_{k3}\Delta\omega_{l3} + \underline{\frac{1}{2}\Delta\omega_{k3}\Delta\omega_{l3}}\right)d\Omega\\ &+\frac{1}{2}\int_{\Omega_m}\Big[\Delta k_{rs} + \frac{1}{2}\left(\Delta\omega_{r3}\tau_{s3} + \omega_{r3}\Delta\tau_{s3}\right.\\ &\left.+\Delta\omega_{s3}\tau_{r3} + \omega_{s3}\Delta\tau_{r3}\right) - \Delta\omega_{r3}\omega_{s3}\delta^s_rK_r\\ &+\underline{\frac{1}{2}(\Delta\omega_{r3}\Delta\tau_{s3} + \Delta\omega_{s3}\Delta\tau_{r3}) - \frac{1}{2}\Delta\omega_{r3}\Delta\omega_{s3}\delta^s_rK_r\Big]}\\ &\times B_{\mathrm{rspt}}\Big[\Delta k_{pt} + \frac{1}{2}(\Delta\omega_{p3}\tau_{t3} + \omega_{p3}\Delta\tau_{t3}\\ &+\Delta\omega_{t3}\tau_{p3} + \omega_{t3}\Delta\tau_{p3}) - \Delta\omega_{p3}\omega_{t3}\delta^t_pK_p\\ &+\underline{\frac{1}{2}(\Delta\omega_{p3}\Delta\tau_{t3} + \Delta\omega_{t3}\Delta\tau_{p3}) - \frac{1}{2}\Delta\omega_{p3}\Delta\omega_{t3}\delta^t_pK_p\Big]}d\Omega\\ &+\int_{\Omega_m} N_{ij}\left(\Delta e_{ij} + \frac{1}{2}\Delta\omega_{i3}\omega_{j3} + \frac{1}{2}\omega_{i3}\Delta\omega_{j3}\right)d\Omega\\ &+\int_{\Omega_m} M_{rs}\Big[\Delta k_{rs} + \frac{1}{2}\\ &\times(\Delta\omega_{r3}\tau_{s3} + \omega_{r3}\Delta\tau_{s3} + \Delta\omega_{s3}\tau_{r3} + \omega_{s3}\Delta\tau_{r3})\\ &-\Delta\omega_{r3}\omega_{s3}\delta^s_rK_r]d\Omega\\ &-\int_{\Omega_m}(q_i+\Delta q_i)\Delta u_i d\Omega - \int_{\Omega_m}(p_r+\Delta p_r)\Delta\gamma_r d\Omega\\ &-\int_{\Gamma_{m\sigma}}(\tilde N^*_{ni} + \Delta\tilde N^*_{ni})\Delta u_i d\Gamma\\ &-\int_{\Gamma_{m\sigma}}(\tilde M^*_{nr} + \Delta\tilde M^*_{nr})\Delta\gamma_r d\Gamma \;\rightarrow\; \min;\\ &\qquad i,j,k,l = 1,2,3; r,s,p,t = 1,2. \end{aligned} \tag{7}$$

The forces and moments in the shell are found from:

$$N_{rr} = \int_{-h/2}^{h/2}\sigma_{rr}(1+\alpha_3K_s)d\alpha_3; r,s=1,2; r\neq s;$$

$$N_{12} = \int_{-h/2}^{h/2}\sigma_{12}d\alpha_3$$

$$N_{r3} = N_{3r} = \int_{-h/2}^{h/2}\sigma_{r3}(1+\alpha_3K_s)d\alpha_3;\ r,s=1,2;\ r\neq s;$$

$$M_{rr} = \int_{-h/2}^{h/2} \sigma_{rr}(1+\alpha_3 K_s)\alpha_3 d\alpha_3;$$

$$r,s = 1,2; \quad r \neq s; \quad M_{12} = \int_{-h/2}^{h/2} \sigma_{12}\alpha_3 d\alpha_3$$

where $\sigma_{rr}, \sigma_{12}, \sigma_{r3}$ are the elements of the second (symmetric) Piola-Kirchhoff tensor. The quantities N_{ij} and M_{rs} are related with Green's strains ε_{kl} and κ_{pt} by:

$$N_{ij} = A_{ijkl}\varepsilon_{kl} \quad M_{rs} = B_{rspt}\kappa_{pt}$$

where:

$$\begin{gathered} A_{rrrr} = \frac{Eh}{1-\nu^2}, \quad A_{rrss} = \frac{\nu Eh}{1-\nu^2}, \\ A_{rsrs} = A_{rssr} = \frac{Eh}{2(1+\nu)}, \\ A_{r3r3} = A_{r33r} = A_{3rr3} = A_{3r3r} = 5/6 G'h, \\ B_{rrrr} = \frac{Eh^3}{12(1-\nu^2)}, \quad B_{rrss} = \frac{\nu Eh^3}{12(1-\nu^2)}, \\ B_{rsrs} = B_{rssr} = \frac{Eh^3}{24(1+\nu)}, \quad r,s = 1,2; \quad r \neq s. \end{gathered} \tag{8}$$

Functional (7) contains terms of the third and fourth order with respect to the unknown functions. An iterative "continuous" Newton's procedure will be used for minimisation of this functional. Assume that the increments $\Delta q_j, \Delta p_r, \Delta\tilde{N}^*_{nj}, \Delta\tilde{M}^*_{nr}$ are given, and known are the approximations $\Delta u_j^{(i)}, \Delta\gamma_r^{(i)}$ of the functions to be found. Let the exact solution be presented in the form:

$$\Delta u_j = \Delta u_j^{(i)} + \delta u_j^{(i)}, \Delta\gamma_r = \Delta\gamma_r^{(i)} + \delta\gamma_r^{(i)}. \tag{9}$$

It is assumed that $\delta u_j^{(i)}, \delta\gamma_r^{(i)}$ are less by couple orders than $\Delta u_j^{(i)}$ and $\Delta\gamma_r^{(i)}$. Let functional (7) be expressed in terms of $\delta u_j^{(i)}, \delta\gamma_r^{(i)}$. For this purpose $\delta u_j^{(i)}, \delta\gamma_r^{(i)}$ are to be replaced with $u_j^{(i)} + \Delta u_j^{(i)}$, $\gamma_r^{(i)} + \Delta\gamma_r^{(i)}$ and $q_j, p_r, \tilde{N}^*_{nj}, \tilde{M}^*_{nr}$ with $q_j + \Delta q_j, p_r + \Delta p_r$. Any Δ – quantity should be exchanged with δ – ones, and $\delta q_j, \delta p_r, \delta\tilde{N}^*_{nj}, \delta\tilde{M}^*_{nr}$ assumed zero. All terms of the $(\delta u)^3, (\delta u)^4$ order are to be neglected in the functional, afterwards. As a result, the square functional $\bar{L}^\delta(\delta u, \delta\gamma)$ is obtained. It can be easily minimised by making use of one of the known Ritz methods.

In order to solve the deformation problem of the shell in the non-linear range, FEM procedures developed for linear problems will be adopted. To this end, the surface Ω will be presented in the form of M curvilinear quadrangles Ω_e with eight nodal points at the boundaries. Let map the interior of the square $\Xi = \{\varsigma_1, \varsigma_2 : -1 \leqslant \varsigma_i \leqslant 1\}$ onto the area Ω_e by the following transformation:

$$\alpha_p = \sum_{\substack{k,j=-1,0,1 \\ k^2+j^2\neq 0}} \alpha_{pkj}\Phi_{kj}(\varsigma_1, \varsigma_2); \quad p = 1,2;$$

where the square base functions Φ_{kj} are given by:

$$\Phi_{kj} = -\frac{1}{4}(1+k\varsigma_1)(1+j\varsigma_2)(1-k\varsigma_1 - j\varsigma_2),$$

$$\Phi_{0j} = \frac{1}{2}(1-\varsigma_1^2)(1+j\varsigma_2),$$

$$\Phi_{k0} = \frac{1}{2}(1+k\varsigma_1)(1-\varsigma_2^2), \quad k,j = -1,1;$$

where $(\alpha_{1kj}, \alpha_{2kj})$ are the co-ordinates of the (k,j)-th node of the element Ω_e. The unknown functions $\delta u_j^{(i)}, \delta\gamma_r^{(i)}$ are defined in the standard element Ξ as follows:

$$\delta u_j^{(i)} = \Phi(\varsigma_1, \varsigma_2)c_j^{(ei1)}, \delta\gamma_r^{(i)} = \Phi(\varsigma_1, \varsigma_2)c_r^{(ei2)}. \tag{10}$$

where the square base functions Φ_{kj} are:

$$\Phi(\varsigma_1, \varsigma_2) = [\Phi_{-1,-1}\Phi_{0,-1}\Phi_{1,-1}\Phi_{1,0}\Phi_{1,1}\Phi_{0,1}\Phi_{-1,1}\Phi_{-1,0}];$$

$$c_j^{(ei1)}, c_r^{(ei2)}.$$

where

$$\Phi(\varsigma_1, \varsigma_2) = [\Phi_{-1,-1}\Phi_{0,-1}\Phi_{1,-1}\Phi_{1,0}\Phi_{1,1}\Phi_{0,1}\Phi_{-1,1}\Phi_{-1,0}];$$

$c_j^{(ei1)}, c_r^{(ei2)}$ – denote the matrices of unknown nodal values of the sought functions at the nodal points of the element Ω_e. Starting from the minimum condition on the functional $\bar{L}^\delta(\delta u, \delta\gamma)$ defined on functions (10) and satisfying homogeneous boundary conditions at the boundary $\Gamma_m \backslash \Gamma_{m\sigma}$, one obtains a system of algebraic linear equations:

$$\sum_{e=1}^{M} K^{(ei)}c^{(ei)} = \sum_{e=1}^{M} F^{(ei)}$$

The solution to that system is a set of values of the increments $\delta u_j^{(i)}, \delta\gamma_r^{(i)}$ at the nodal points of the element Ω_e. For finding the $(i+1)$-th approximation of the sought functions $\Delta u_j^{(i+1)}, \Delta\gamma_r^{(i+1)}$ one should add the obtained increments to the known values of $\Delta u_j^{(i)}, \Delta\gamma_r^{(i)}$. The above procedure is continued until the increments $\Delta u_j^{(i)}, \Delta\gamma_r^{(i)}$ satisfy the following condition:

$$\left\|\delta u_j^{(i)}\right\| \leqslant \varepsilon \left\|\Delta u_j^{(i)}\right\|, \quad \left\|\delta\gamma_r^{(i)}\right\| \leqslant \varepsilon \left\|\Delta\gamma_r^{(i)}\right\|$$

3. Exemplary calculations of gear of harmonic drive

Now we determine the stress state in the flexspline and flexible rings of a harmonic drive.

3.1. Determination of the zone of forces acting on the flexspline and flexible bearing of the harmonic drive generator. For a cam generator with a circular deformation curve subject to four forces inclined by $1/2\beta$ with respect to the principal axis and having involute teeth profile with the nominal angle $\alpha = (\pi/9)$ and radial deformation-to-module ratio $w/m = 1.0 - 1.2$, the

tangential component of the loading (see Fig. 1) is given by the following relationship:

$$\bar{P}(X,Y,t)\begin{cases} P_{\max} * \sin^2 \frac{(\beta-\omega\, t)}{\beta_0} * \pi \\ \omega\, t \leqslant \beta \leqslant \beta_0 + \omega\, t \\ P_{\max} * \sin^2 \frac{(\beta-\pi-\omega\, t)}{\beta_0} * \pi \\ \pi + \omega\, t \leqslant \beta \leqslant \pi + \beta_0 + \omega\, t \end{cases} \tag{11}$$

for $X_1 \leqslant X \leqslant X_2$; for the rest $X:\ \bar{p}(x,y,t) = 0$.

$$P_{\max} = f(M_s) \tag{12}$$

where:

$$X_1 = \frac{L_1}{L}, \quad X_2 = \frac{L_2}{L}, \quad \beta = \frac{Y}{R}$$

L – length of the sleeve, R – radius of the middle surface before deformation, ωt – angular displacement measured from the great generator axis.

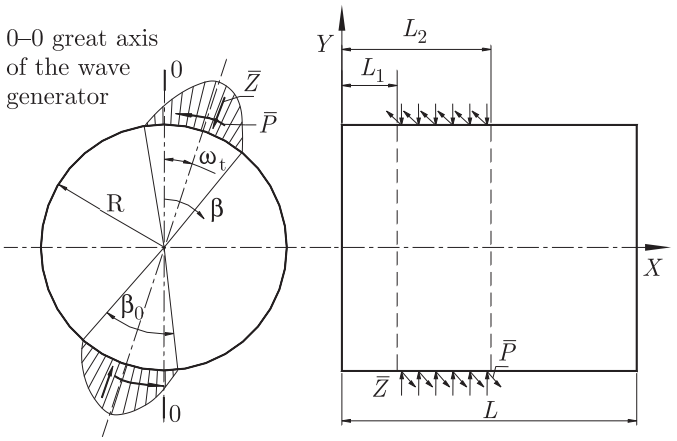

Fig. 1. Distribution of mesh forces assumed in the considered model

According to the above formula, a constant value of the loading $\bar{p}(x,y,t)$ is assumed along the length X. It amounts to the average value of the tangential component of the meshing force along the tooth length. Some considerations on the function of loading, its variability along X, and results of investigations are presented in [8]. The relation between $P_{\max}$ and the transmitted torque M_s is given by:

$$M_s = 2 * \int_{\omega * t}^{\omega * t + \beta_0} b * \left(\frac{d}{2}\right)^2 * P_{\max} * \sin^2 \frac{\pi(\beta - \omega * t)}{\beta_0} d\beta \tag{13}$$

$b = L_2 - L_1$ – width of the flex-gear teeth, d – pitch diameter of the flexspline.

The normal component of the loading in the meshing zone is:

$$\bar{Z}(x,y,t) = P_{\max} * \sin^2 \frac{\pi * (\beta - \omega * t)}{\beta_0} * tg\vartheta_0 \tag{14}$$

where the function and domain of $\bar{Z}(x,y,t)$ are the same as for $\bar{p}(x,y,t)$.

The experimentally found functions of loading variability in both zones in a transverse cross-section and along the tooth length are discussed in work [9]. The normal component is balanced by the generator reaction. The torque due to the tangential component (circumferential) is balanced by the torque M_s in the output shaft. Because of the non-uniform distribution of $\bar{p}(x,y,t)$ over the circumference of the flexspline, this component tends to change the shape of the flexspline. This is opposed by the normal reaction from the generator $\bar{Z}_g$. According to [10], we can put down:

$$\overline{Z}_g = \int \bar{p} d\beta \tag{15}$$

By expressing $\bar{p}(x,y,t)$ in terms of the series:

$$\bar{p} = \bar{p}_0 + \sum_{n=2,4} \bar{p} * n * \sin^2 n * (\beta - \omega * t) \tag{16}$$

and integrating from $\beta = \omega t$ to $\beta = \omega t + 2\pi$, we obtain:

$$\bar{p}_0 = \frac{2}{\pi} * p_{\max} * \int_{\omega * t}^{\omega * t + \beta_0} \sin^2 \frac{\pi(\beta - \omega * t)}{\beta_0} d\beta \tag{17}$$

By multiplying (4.5) by $\sin^2 n(\beta - \omega t)$ and equating the terms of the same n, then integrating over the abovementioned boundaries, we get:

$$\bar{p}_n = \frac{4}{3} * \frac{p_{\max}}{\pi} * \left[2 * \int_{\omega * t}^{\omega * t + \beta_0} \sin^2 \frac{\pi(\beta - \omega * t)}{\beta_0} * \sin^2 n * (\beta - \omega * t)\, d\beta + \beta_0 \right] \tag{18}$$

Since $\bar{p}_0$ is equivalent to the torque M_s in the silent-running shaft, then the change of the flexspline shape is produced by the component $\bar{p}_n$. Hence, the normal reaction of the generator bearing will be:

$$\bar{Z}_g = \int \sum_{n=2,4,\ldots} \bar{p}_n * \sin^2 n * (\beta - \omega * t)\, d\beta = \sum_{2,4,\ldots} \bar{p}_n \times \left[\frac{1}{2}(\beta - \omega * t) + \frac{1}{4n} * \sin 2n * (\beta - \omega * t) \right] + C \tag{19}$$

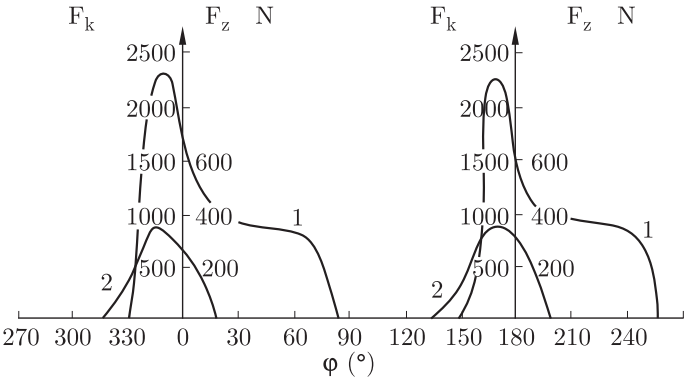

Fig. 2. Distribution of mesh forces – 1, and forces acting on rolling elements of the bearing – 2 (according to experimental investigations)

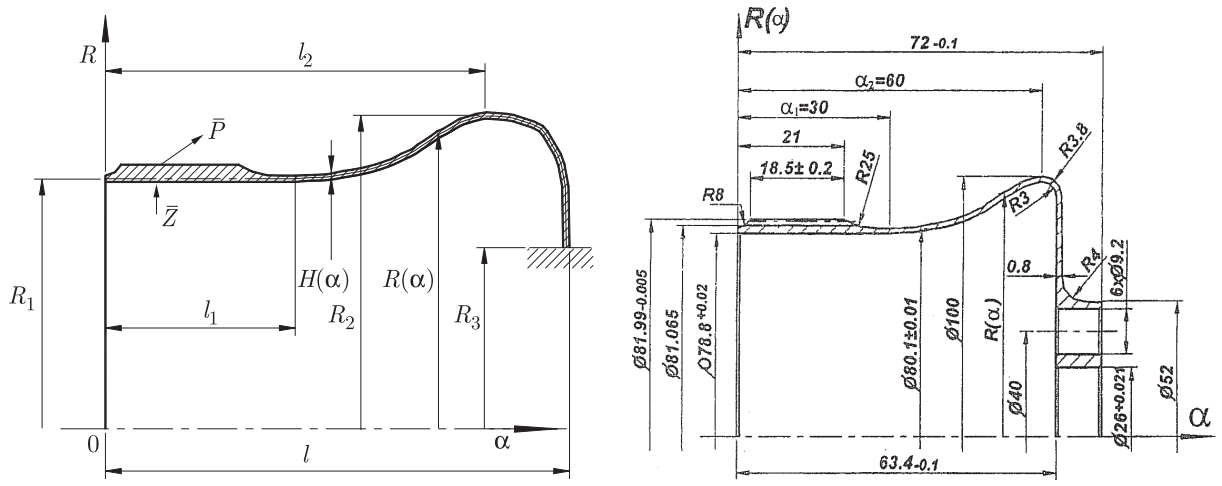

$$\left\{ \begin{array}{c} R = R_1, \quad 0 < \alpha \le \alpha_1 \\ R = R_1 + (R_2 - R_1)\left[1 - 3\left(\dfrac{\alpha_2 - \alpha}{\alpha_2 - \alpha_1}\right)^2 + 2\left(\dfrac{\alpha_2 - \alpha}{\alpha_2 - \alpha_1}\right)^3, \quad \alpha_1 \le \alpha \le \alpha_2\right] \\ R = R_2, \quad \alpha \ge \alpha_2 \end{array} \right\}$$

Fig. 3. Scheme of the flexspline in the optimal harmonic drive

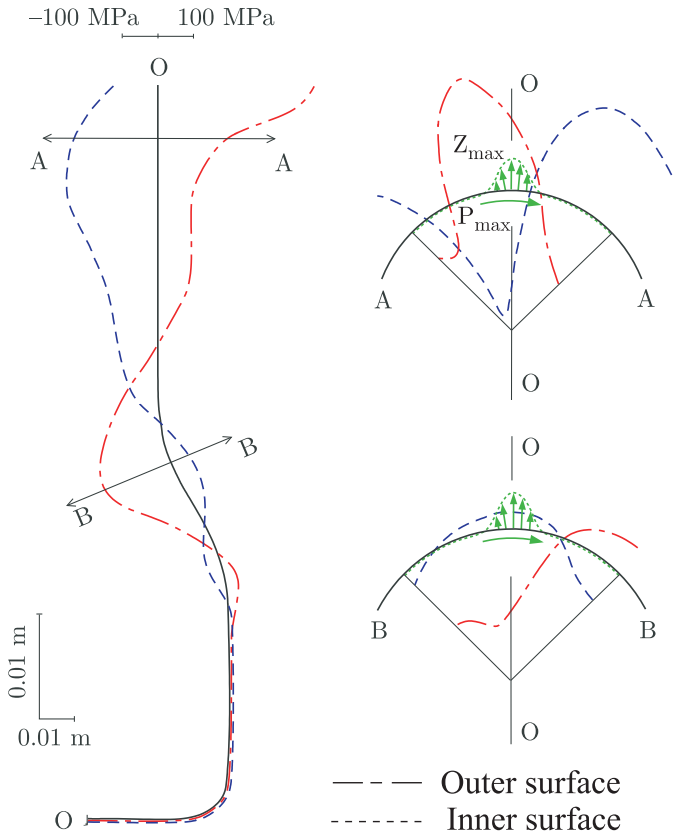

Fig. 4. Circumferential stresses

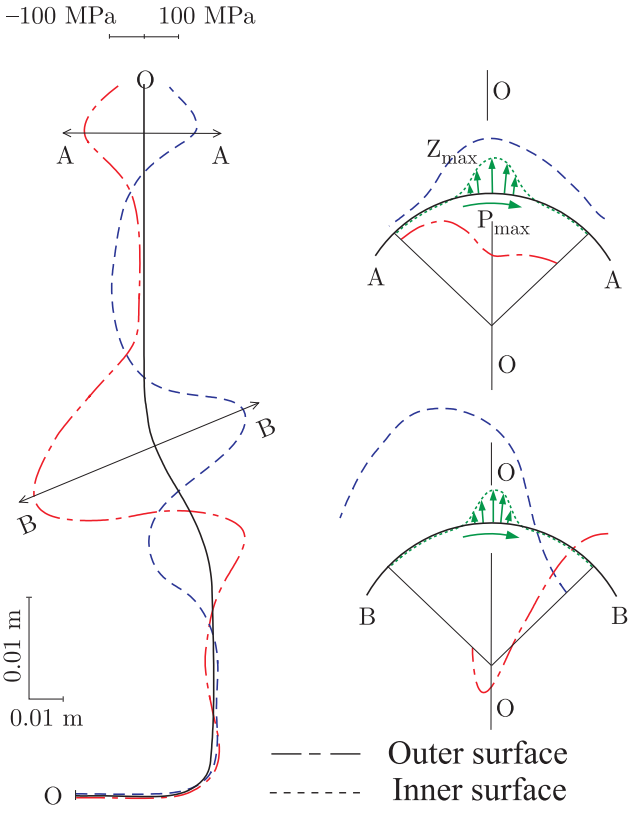

Fig. 5. Axial stresses

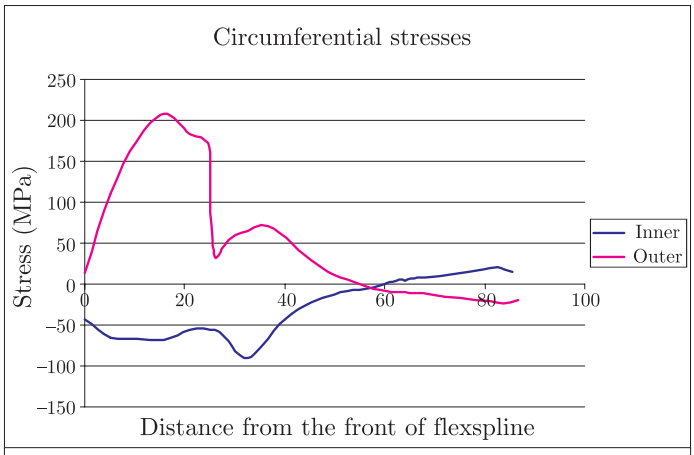

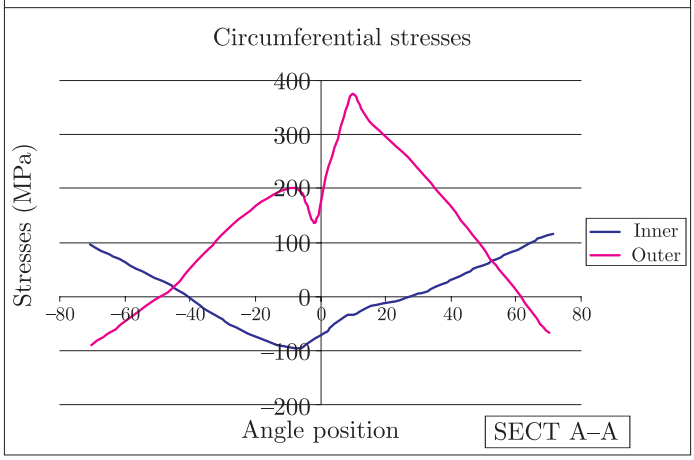

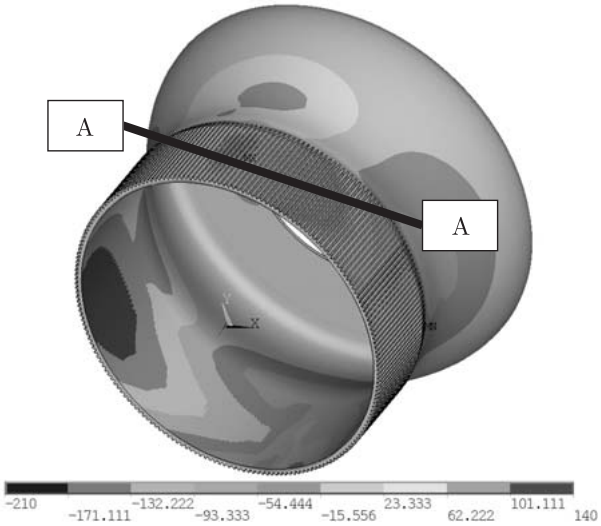

Fig. 6. Circumferential stresses [FEM ANSYS]

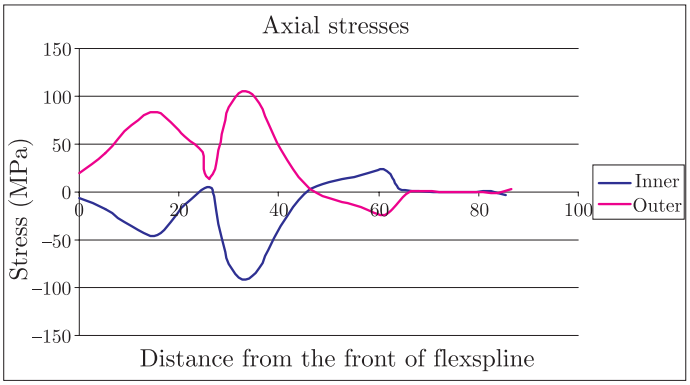

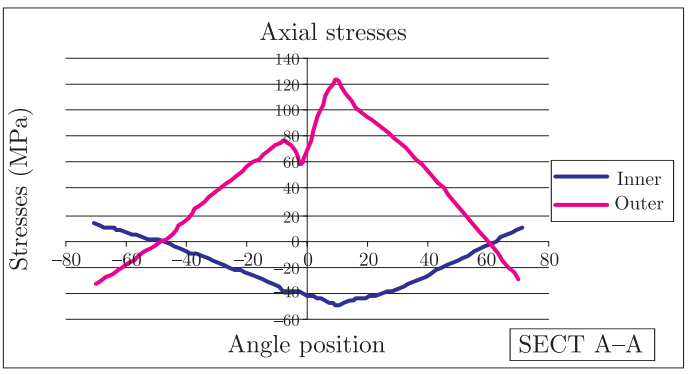

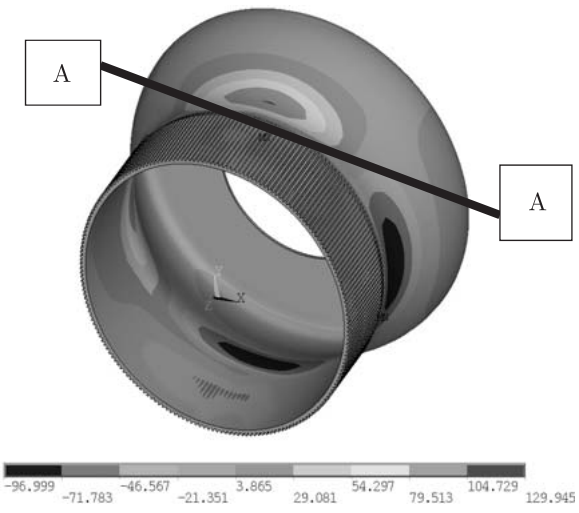

Fig. 7. Axial stresses [FEM ANSYS]

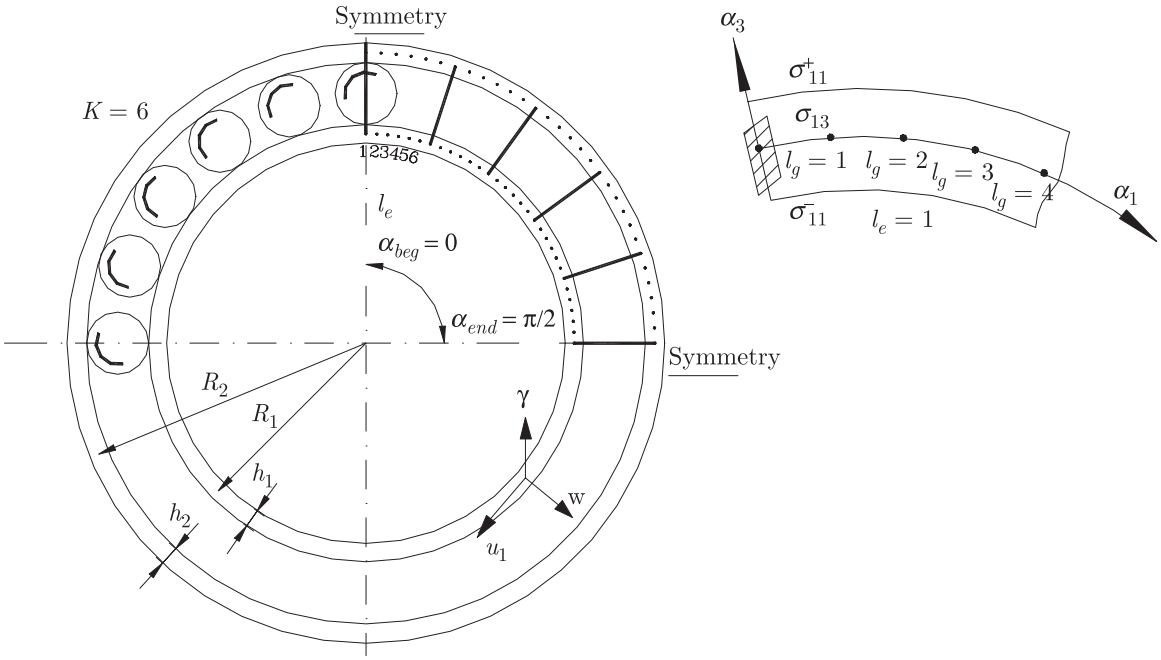

Fig. 8. Scheme of the flexible bearing and its division into finite elements

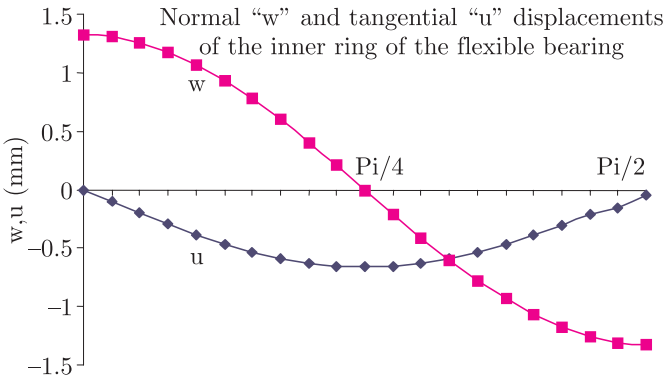

Fig. 9. Displacements of the inner ring of the flexible bearing

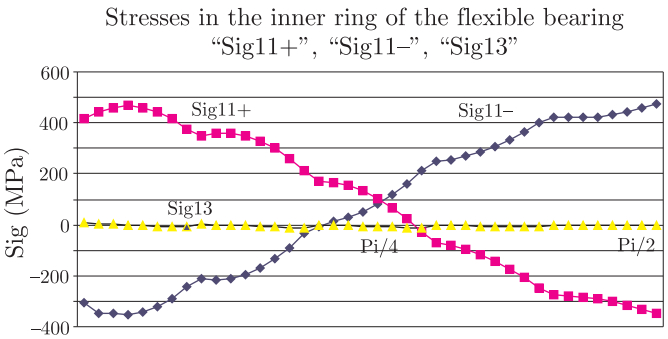

Fig. 11. Stresses in the inner ring of the flexible bearing

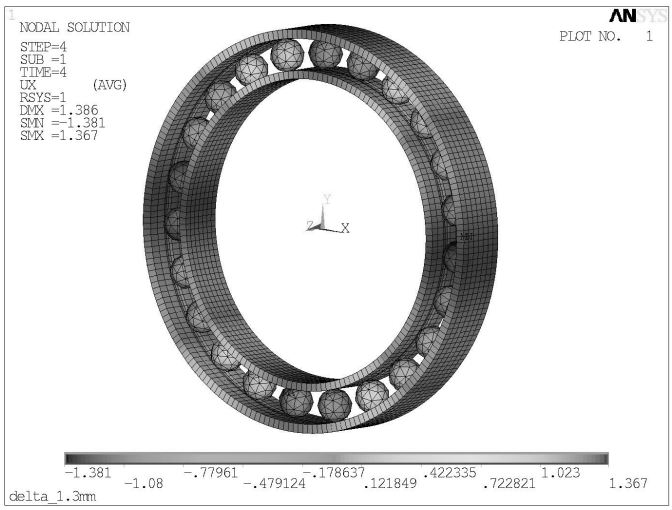

Fig. 10. Displacements of the rings of the flexible bearing [ANSYS]

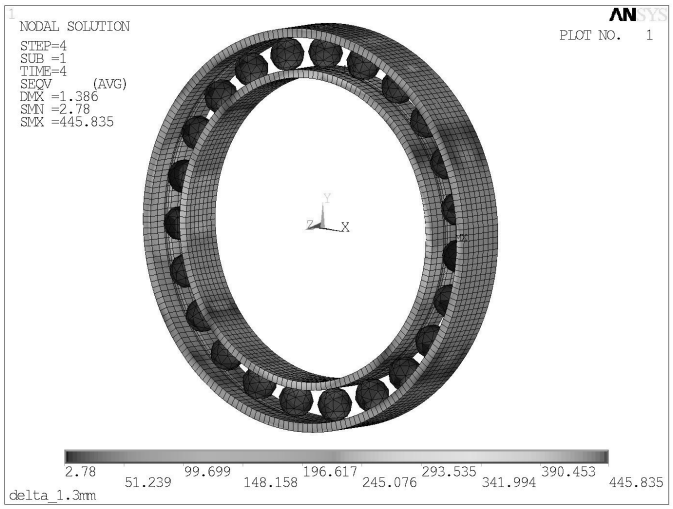

Fig. 12. Stresses in the rings of the flexible bearing [ANSYS]

where:

$$C = -\sum_{2,4,\ldots} \frac{\bar{p}_n}{n} \times \left[\frac{n}{2}\left(H^* - \omega * t\right) + \frac{1}{4} * \sin 2n * \left(H^* - \omega * t\right)\right] + C$$

which ensues from the condition of unilateral contact ($\bar{Z}_g \geqslant 0$), where H^* is the value of the angle β for which the expression $\sum_n \bar{p}_n[\ldots]$ in Eq. (19) reaches the global minimum [11]. Finally, the tangential component of loading acting on the flexspline from the toothed side, given by (11), and the normal one, (14) and (19), is defined as:

$$\bar{Z}_s = \bar{Z} + \bar{Z}_g \tag{20}$$

3.2. Numerical results. For the improvement of conditions of operation between toothed rings in harmonic drives as well as for the lowering of maximum stresses in the flexible shell, a variable-curvature flexspline design has been proposed [12]. Its scheme is shown in Fig. 3. The stress state in such a structural solution can be determined by making use of the proposed FEM procedure.

The boundary conditions of the flexible sleeve shown in Fig. 3 are as follows: one edge clamped, the radial and circumferential forces given by formulas (14) and (19) and (11) are applied to the other edge. The meshing in a part of the flexspline is reflected by a local increase in the thickness of the smooth sleeve, equivalent to the average radial stiffness of the flexspline. For elimination of difficulties brought about by non-linear effects, the whole structure is treated as a sum of partial elements. Each element is described by the corresponding stiffness matrix and load vector. The solution to the complete set of algebraic equations (linear ones) is obtained on the grounds of a transection algorithm (subsequent section of the structure) and formulation of 'gluing' matrices. In Figs. 4 and 5, diagrams of circumferential and axial stresses (on the inner and outer surfaces) along the sleeve generatrix are presented, respectively. Calculations have been made for the following data: $L = 0.07$ m, $h = 0.001$ m, $R1 = 0.04$ m, $R2 = 0.06$ m, $R3 = 0.02$ m, $\beta_o = \frac{\pi}{8}$, $M_s = 100$ Nm, material of the sleeve: 40 HMN. The obtained results are in good agreement with those found with the help of the FEM ADINA procedure [12].

Basing on the above mentioned methodology, a computer program has been worked out, which enabled determination of the stress state in the rings of an exemplary flexible bearing loaded by the forces as indicated in Section 2.

Below a scheme of division of the flexible bearing into finite elements as well as the results of calculations from the linearised formulation (denotations as in Fig. 8) are presented.

4. Conclusions and remarks

The proposed finite element method has been used for determination of stresses in the harmonic flexible ring as well as stress and strain states in the internal ring of the flexible bearing of the wave generator.

Analysis of stresses In the flexspline of the considered harmonic driver with variable curvature determined by the proposed method [OM] and via ANSYS (see Figs. 4–7) leads to following conclusions:

- circumferential stresses in the cross-section on the outer side in the middle of the flexspline length have maxima $\sigma_{OM} = 325$ MPa, $\sigma_{ANSYS} = 360$ MPa (according to both methods), which are shifted with respect to the generator axis by 200 and 160, respectively,
- the same two methods yield maximum stresses on the inner side of different values but the same sign. Qualitatively, the axial distributions of these stresses are similar, quantitatively – definitely divergent.

The discrepancy is brought about by the fact that the flexible sleeve has been loaded in the meshing zone by forces described by formulas set forth in Section 3.1 for the given boundary conditions. The meshing zone has been modelled as a smooth sleeve with an increased thickness and average stiffness due to teeth. In the ANSYS approach, though, the meshing zone has been fully modeled together with contact between the sleeve and flexible bearing of the generator (which made the whole model more realistic).

In the case of examinations of the flexible bearings only, the results coincide more (Figs. 9–12). In both methods, the loadings from the sleeve side and kinematic excitations from the generator cam have been assumed the same. ANSYS has been chosen for the calculations in this paper, since it is a professional and very popular tool for analysis of complex systems undergoing mechanical and thermal loadings with multiple areas of contact taken into account.

It should be emphasized that the proposed method enables one to find a solution to the given task until the first critical point is reached, i.e. a point in the parameter space around which the calculation procedure becomes unstable because of ambiguity in the relation between deformation and loading.

References

[1] J.T. Oden, *Finite Elements Of Nonlinear Continua*, Mc Graf-Hill Book Comp., New York, 1972.

[2] J.G. Sawula, Priedstawlenije sredinnych powierchnostej obolocek reznymi powierchnostiami, *Prikl. Mechanika* 20 (12), 70–75 (1984), (in Russian).

[3] J. Grigorenko and W.I. Gulajew, "Nieliniejnyje zadaci teorii obolocek i metody reszenia", *Prikl. Mechanika* 27 (10), 3–23 (1991), (in Russian).

[4] W. Pietraszkiewicz, "Non-linear theories of thin elastic shells", *Proc. Polish. Symp. Shell Structures, Theory and Aplications*, 27–50 (1978).

[5] R.F. Kao, "Comparison of Newton-Raphson methods and incremental procedures for geometrically nonlinear analysis", *Comp. & Struc.* 4, 1091–1097 (1974).

[6] P.V. Marcal, "Large defection analysis of elastic-plastic shells of revolution", *AIAA* 8, 1627–1633 (1970).

[7] I.S. Mukha, "Issliedowanije uprugowo deformirowanija sostawnych gibkich tiel metodom koniecznych elementow, *Wiestnik Lviv. Uniw-taSer. Mech.-mat.* 46, 35–42 (1997), (in Russian).

[8] D.P. Volkov and A.R. Krajniev, *Planetary Gear Systems and Harmonic Drives of Road and Building Machinery*, Mashinostroenie, Moscow, 1968, (in Russian).

[9] V.A. Finogenev and M.N. Ivanov, "Harmonic drives", *Tesisy Dokladov Vsesojuznogo Simposjuma, Niekotorye Resultaty Kompleksnych Eksperymentov i Issledovanij*, 1973, (in Russian).

[10] S.V. Bojarsijnov, *Fundamentals of Buildings Mechanics*, Mashinostroenie, Moscow, 1973, (in Russian).

[11] M. N. Ivanov, *Harmonic Gear Drives*, Moscow, 1981, (in Russian).

[12] W. Ostapski, "Engineering design of harmonic drive gearings towards quality criteria", *Machine Dynamics Problems* 21, (1998).